scientific reports

Check for updates

OPEN

Measuring and modeling the solubility of sulfasalazine in supercritical carbon dioxide to select methods for producing nanoparticles

Yahia Alghazwani[1], Mohammed Ghazwani[5], Sirajunisa Talath[2], Adil Farooq Wali[2], Sathvik B. Sridhar[3], Farhat Fatima[4] & Umme Hani[5]✉

In the present study, the solubility of sulfasalazine in carbon dioxide was investigated at temperatures ranging from 313 K to 343 K and pressures ranging from 12 to 30 MPa. The experimentally determined molar solubilities of sulfasalazine in $ScCO_2$ were found to be in the range of 4.08×10^{-5} to 8.61×10^{-5} at 313 K, 3.54×10^{-5} to 11.41×10^{-5} at 323 K, 3.04×10^{-5} to 13.64×10^{-5} at 333 K, and 2.66×10^{-5} to 16.35×10^{-5} at 343 K. The solubility values were correlated via a number of different types of equations, such as semi-empirical correlations, the Peng-Robinson, the PC-SAFT equation, and the regular solution. Furthermore, the findings demonstrate that semi-empirical, equation of state models, and the regular solution model possess the capability of precisely determining the solubility. Moreover, the solubility magnitude suggests that the gas anti-solvent method may be a viable approach for nanoparticle production.

Keywords Sulfasalazine, Solubility, Modeling, Supercritical fluid, PC-SAFT

List of symbols

$\mathbf{a_0}-\mathbf{a_4}$	The model adjustable parameters
$\mathbf{AARD\%}$	Average absolute relative deviation
$\mathbf{a\ (T)}$	Parameter of the EoS ($Nm^4\ mol^{-2}$)
$\mathbf{\overset{?}{a}}$	Helmholtz free energy
$\mathbf{b}$	Parameter of the EoS ($m^3\ mol^{-1}$)
k	Boltzman constant, $J\ K^{-1}$
$\mathbf{k_{ij}}$	Binary interaction parameter in the mixing rules
$\mathbf{l_{ij}}$	Binary interaction parameter in the mixing rules
$\mathbf{N}$	Number of data points, dimensionless
N_f	Number of fitted parameters
$\mathbf{P}$	Pressure
$\mathbf{P_c}$	Critical pressure
$\boldsymbol{P_r}$	Reduced pressure
$\boldsymbol{P_{ref}}$	Reference pressure
$\mathbf{P_{sub}}$	Sublimation pressure (Pa)
$\mathbf{Q}$	Number of independent variables
$\mathbf{R}$	Gas constant, $Jmol^{-1}\ K^{-1}$
$\mathbf{R^2}$	Correlation coefficient
$\mathbf{R_{adj}}$	Adjusted correlation coefficient

[1]Department of Pharmacology, College of Pharmacy, King Khalid University, Abha, Saudi Arabia. [2]Department of Pharmaceutical Chemistry, RAK College of Pharmacy, RAK Medical & Health Sciences University, Ras Al Khaimah, Ras Al Khaimah, UAE. [3]Department of Clinical Pharmacy & Pharmacology, RAK College of Pharmacy, RAK Medical & Health Sciences University, Ras Al Khaimah, United Arab Emirates. [4]Department of Pharmaceutics, College of Pharmacy, Prince Sattam bin Abdulaziz University, Al- Kharj 11942, Saudi Arabia. [5]Department of Pharmaceutics, College of Pharmacy, King Khalid University, Abha, Saudi Arabia. ✉email: uahmed@kku.edu.sa

$\mathbf{S}$	Equilibrium solubility
$\mathbf{T}$	Temperature, K
$\mathbf{T_b}$	Boling point
$\mathbf{T_c}$	Critical temperature
$\mathbf{T_r}$	Reduced temperature
$\mathbf{y}_2$	Mole fraction solubility
v^s	Solid molar volume
$\mathbf{vdW2}$	Van der Waals mixing rule with two adjustable parameters
$\mathbf{Z}$	Compressibility factor

Greek symbols

$\boldsymbol{\alpha}\ (\boldsymbol{T_r},\ \boldsymbol{\omega}\ )$	parameter of the EoS, Temperature-dependent
ε	Depth of pair potential, J
η	Packing fraction
$\boldsymbol{\rho}$	Density, kg m^{-3}
$\boldsymbol{\sigma}$	Segment diameter, Å
$\varnothing$	Fugacity coefficient
$\boldsymbol{\omega}$	Acentric factor

Superscripts

cal	Calculated
disp	Contribution due to dispersive attraction
exp	Experimental
hc	Residual contribution of hard-chain system
hs	Residual contribution of hard-sphere system
i, j	Component
l	Liquid
s	Solid
scf	Supercritical fluid

Subscripts

i, j	Component
c	Critical property
2	Solute

Sulfasalazine, an anti-inflammatory drug utilized to treat rheumatoid arthritis and ulcerative colitis, was initially identified in the 1930s. The drug under consideration is classified as a class 4 compound in accordance with the Biopharmaceutical Classification System, primarily due to its restricted solubility (0.6 µg/ml) and permeation properties. Consequently, a recommended daily oral dose of 1–3 g/day has been established for patients with arthritis to compensate for the low level of exposure. Moreover, the low permeability and solubility of sulfasalazine would present considerable obstacles to achieving a considerable level of exposure following intravenous administration. This is due to the limited volume of doses that can be administered. It is therefore of great importance to enhance the APIs through the creation of diverse drug formulations. This objective can be met by undertaking a detailed examination of the physicochemical characteristics of sulfasalazine, with a particular focus on its solubility and distribution within the selected solvents[1].

Solubility represents a pivotal parameter that significantly impacts the absorption of oral drugs from the stomach and intestines. During the initial stages of drug discovery, solubility is a valuable parameter when considered alongside other properties, including ionization, lipophilicity, and permeability. In the later stages of drug development, it is also essential in classifying biopharmaceuticals, optimizing formulations, and designing a novel drug formulation[2].

Reducing the particle size of APIs is an effective method for improving solubility in poorly soluble APIs. Conventional techniques have limitations, including difficulty controlling particle size, the presence of solvent in the finished API, and potential degradation due to heating. Supercritical fluid technology is a promising approach for developing particle reduction technology for pharmaceuticals[3–7]. A number of effective supercritical fluid techniques have been established for reducing particle size in drugs. The key factor in choosing the right supercritical fluid technique is understanding how the drug dissolves in supercritical carbon dioxide ($ScCO_2$). To industrialize and commercialize products derived from supercritical fluid (SCF) processes, it is essential to gain comprehensive knowledge of the quality, purity, extractability, and solubility of these materials.

Mathematical and experimental models have played a pivotal role in reducing the cost of solubility tests. By modeling solubility, we can accurately determine experimental measurements and investigate various aspects of thermodynamics and material properties. In the present era, we have advanced experimental models, equations of state, and intelligent models to achieve this objective. Accordingly, the solubility of sulfasalazine in $ScCO_2$ was determined under a range of temperature and pressure condition. The data were then subjected to modeling using a variety of techniques, including (1) density-based models, (2) PR with vdW2, (3) PC-SAFT, and (4) the regular solution model. Subsequently, the potential of semi-empirical models for the analysis of the data was explored. Furthermore, an assessment was conducted to evaluate the capacity of the models to be correlated. This involved a comparison between the calculated data and the experimental data, with the aim of identifying any potential discrepancies. Two statistical criteria were employed to assess the models' capabilities: the average absolute relative deviation (AARD) and the adjusted correlation coefficient (R_{adj}). Following this analysis, the enthalpies of vaporization (ΔH_{vap}), solvation (ΔH_{sol}), and total enthalpy (ΔH_{total}) were determined.

Materials and methods

Materials

Sulfasalazine with below structure (Fig. 1) (CAS number 599-79-1) was procured from Sigma-Aldrich, while CO_2 of greater than 99.5% purity was obtained from a local supplier.

Methods

Experimental procedure

The solubility of sulfasalazine in supercritical carbon dioxide was evaluated according to the procedure reported in previous articles[8,9]. The initial stage of the experiment involved directing a CO_2 gas with a pressure of 5.5 MPa and a temperature of 298 K to a refrigerator with a temperature of 268 K, with the objective of observing the phase transition from gas to liquid. Subsequently, the liquid is subjected to pressure through a specialized pump in order to attain the targeted pressure range (12 to 30 MPa). A high-pressure stainless steel cell with a volume of 200 ml has been constructed for the purpose of conducting solubility experiments. The fixed value of API is recorded on the sheet and positioned at the base of the cell. Subsequently, the liquid is introduced into the cell, where the drug is mixed and dissolved in the carbon dioxide using a high-speed stirrer. The temperature of the process is set as the second impact parameter on solubility using an accurate temperature-control device with a precision of ± 1 K. Based on preliminary experiments; a static time of 4 h with a stirring rate of 200 rpm was identified as sufficient to achieve equilibrium. Finally, the drug mole fraction was determined by applying the following equation using the initial and final drug masses as variables:

$$m_e = m_i - m_f \tag{1}$$

$$\text{Mole of drug} = \frac{m_e}{M_{w,drug}} \tag{2}$$

$$y = \frac{\text{Mole of Drug}}{(\text{Mole of drug} + \text{Mole of } CO_2)} \tag{3}$$

Semi-empirical models

A plethora of semi-empirical models have been put forth with the aim of establishing a correlation between the solubility of a solute in $scCO_2$. The absence of a requirement for solute properties (in contrast to the EoSs), the ease of application, and the acceptable accuracy are the principal advantages of these models. The sole disadvantage of these models is the necessity for experimental solubility data. A number of equation have been formulated with varying adjustable parameters (ranging from three to eight) with the objective of enhancing the correlation with experimental data. As example, Bartle et al.[10], MST[11,12], Chrastil[13], Kumar and Johnston[14], Garlapati et al.[15,16], Alwi and Garlapati[17], del Valle and Aguilera[18], Sung and Shim[19], Adachi and Lu[20], Bian et al.[21,22], Sparks et al.[23], Si-Moussa et al.[24], Belghait et al.[25] and Amooey[26], Haghbakhsh et al.[27], Mitra and Wilson[28], Reddy et al.[29,30], Gordillo et al.[31], sodeifian et al.[32–34] have been put forth as a means of correlating the solubility of solutes in supercritical carbon dioxide. In contrast to the EoSs, there is no necessity to consider the properties of the solute, the method of application is uncomplicated, and the accuracy is satisfactory. The only disadvantage associated with these models is that they necessitate the availability of experimental solubility data[35–38]. The density-based models are founded upon the tenet of straightforward error minimization. The

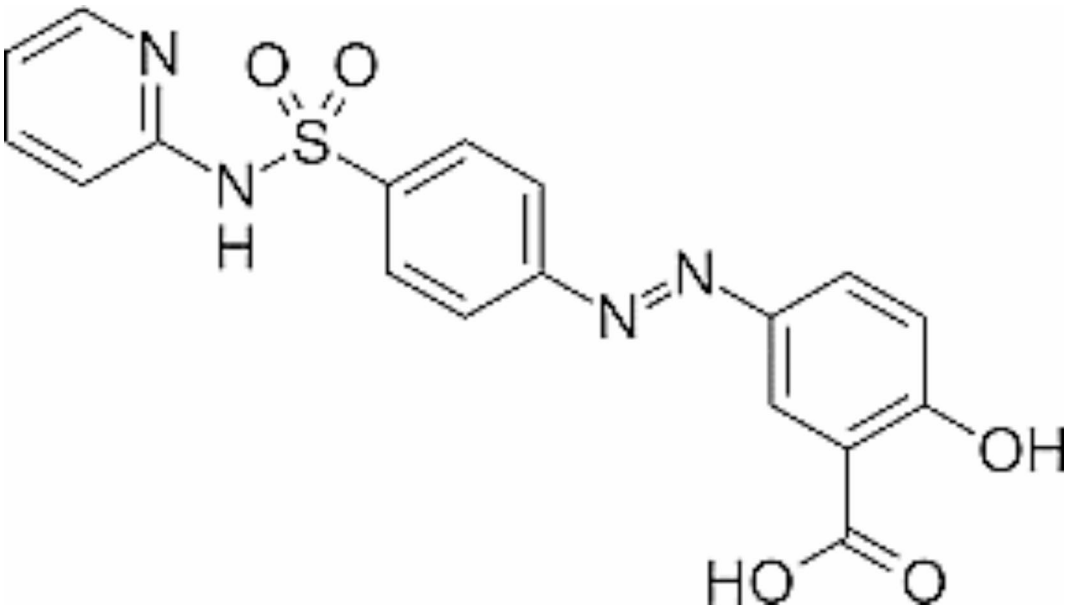

Fig. 1. Structure of sulfasalazine.

adjustable parameters of these models can be optimized by an algorithm, such as a genetic algorithm or simulated annealing, within the MATLAB software. As shown in Table 1, five of the most popular theory-based models were used in this work to estimate data consistency and values of solvation, evaporation, and total enthalpies.

Equation of state-based models

Although the use of thermodynamic models requires a lot of information about the solvent, many authors used these types of models[40–47]. The solubility in $scCO_2$ can be modeled using a variety of techniques, including semi-empirical equations, statistical models, and theoretical frameworks. Nevertheless, the conventional methodology based on the equation of state, exemplified by the Peng-Robinson (PR) and Soave-Redlich-Kwong (SRK) models, frequently yields considerable discrepancies[48–50]. In such cases, it is necessary to utilize the solid properties, which in some instances, particularly for complex solids, may not be readily accessible in a database. Mixing rules (e.g., van der Waals mixing rules) must be employed to ascertain the appropriate parameters by adjusting experimental solubility data in order to minimize this discrepancy. The precision of the EoS is contingent upon the specific mixing rule utilized and the number of parameters.

The use of these types of models necessitates the input of molar volume, acentric factor, melting temperature of solute, solvent vapor pressure, critical properties of the solvent, and thermodynamic properties of carbon dioxide. A plethora of experimental methodologies have been devised to identify these substances, each of which is susceptible to error. Among the most significant methods are the Joback et al.[51], Marrero and Gani[52], Lee Kessler[53], Fedors[54], and Stein et al.[55] methods. In recent years, models such as the Peng Robinson, and SRK models have been employed for drugs such as lsomeprazole[56], loratadine[57], sunitinib malate[58], and pregabalin[8]. The results and output of the articles indicate that, despite the numerous difficulties encountered in their use, these methods have yielded remarkable results on a consistent basis.

Moreover, the SAFT equations represent an additional class of models that have been utilized to establish correlations between the solubility of substances in supercritical carbon dioxide. These models encompass a range of variants, including SAFT, PC-SAFT, SAFT-VR, qCPA, and PCP-SAFT. In comparison to other equations of state, they are more complex in their structure. Consequently, the general or partial forms of these models have been employed in numerous published works[59–66]. The most important point in using these types of models is the molecular relationship between carbon dioxide and the solutes, which many works consider these parameters as adjustable parameters.

To ascertain the solubility of a particular compound in a supercritical state, it is essential to establish a solid-CO_2 equilibrium. This procedure can be represented by means of the fundamental equilibrium relationship between a solid and $ScCO_2$ in a system.

$$f_s^{solid} = f_s^{scCO_2} \tag{4}$$

On the basis of certain simplifying assumptions, the mole fraction is calculated using the following Eqs[67,68]:

$$y_s = \frac{P_s^{sub}(T).\varphi_s^{sat}}{P.\varphi_s} \exp[\frac{\nu_s(P - P_s^{sub}(T))}{RT}] \tag{5}$$

In this context, the solute fugacity coefficient at ϕ_s^{sat} and ϕ_s represents the sublimation pressure of the APIs, which is generally low. Therefore, it can be assumed that ϕ_s^{sat} is equal to one. In order to model an equilibrium process, the value of ϕ_s^{sat} is determined using an appropriate model. To assess the EoSs, the PR and PC-SAFT models were considered.

PC-SAFT model

The PC-SAFT model is formulated based on the residual molar Helmholtz energy (a^{res}) including the, which is the main basis of this model in the present work[69]:

$$\tilde{a}^{res} = A/NKT = \tilde{a}^{hc} + \tilde{a}^{disp} \tag{6}$$

In accordance with the tenets of first-order thermodynamic perturbation theory, the term " a^{hc}" is defined as follows:[62]:

Model	Function
Chrastil[13]	$\ln y = a + b \ln \rho + \frac{c}{T}$
Bartle et al.[39]	$\ln \frac{y.P}{P_{ref}} = a + b(\rho - \rho_{ref}) + \frac{c}{T}$
Kumar- Johnston	$\ln y = a + b\rho + \frac{c}{T}$
Mendez-Santiago and Teja	$T \ln(y.P) = a + b\rho + cT$

Table 1. Semi-empirical models.

$$\tilde{a}^{hc} = (\sum_{i=1}^{N} y_i m_i)\tilde{a}^{hs} - \sum_{i=1}^{N} y_i\,(m_i - 1)\,ln g_{ii}^{hs}\,\sigma_{ii} \tag{7}$$

In addition, the term a^{disp} is calculated by the below relationship[62]:

$$\tilde{a}^{disp} = -2\pi \underbrace{\frac{6}{\pi}\eta\left(\sum_{i=1}^{N} y_i m_i d_i^3\right)^{-1}}_{\rho}\left[l_{1,xk}\overline{m^2\varepsilon\sigma^3} + l_1\overline{(m^2\varepsilon\sigma^3)_{xk}}\right] - \pi\frac{6}{\pi}\eta\left(\sum_{i=1}^{N} y_i m_i d_i^3\right)^{-1} \tag{8}$$
$$\left\{[m_k C_1 l_2 + \bar{m}C_{1,xk}l_2 + \bar{m}C_1 l_{2,xk}] \times \overline{m^2\varepsilon^2\sigma^3} + \bar{m}C_1 l_2\overline{(m^2\varepsilon^2\sigma^3)_{xk}}\right\}$$

In order to ascertain the two cross parameters (ϵ_{ij} and σ_{ij}) the conventional combination rules are employed[62]:

$$\sigma_{ij} = \frac{1}{2}(\sigma_i + \sigma_j) \tag{9}$$

$$\epsilon_{ij} = \sqrt{\epsilon_i \epsilon_j}\,(1 - k_{ij}) \tag{10}$$

In the aforementioned relationship, K_{ij} represents an adjustable parameter that is dependent on temperature. The incorporation of this parameter into the relationship is intended to account for the interactions between the two disparate chains. The correlation between the compressibility factor (Z) and $\tilde{a}^{res}$ can be defined as follows[62]:

$$Z = 1 + \eta\left(\frac{\partial\tilde{a}^{res}}{\partial\eta}\right)_{T,x_i} = 1 + Z^{hc} + Z^{disp} \tag{11}$$

In this context, the dimensionless volume parameter, denoted by the symbol η, is defined as follows:

The fugacity coefficient of component k (ϕ_k) is ultimately established through the following methodology[62]:

$$ln\varphi_k = \tilde{a}^{res} + (Z-1) + \left(\frac{\partial\tilde{a}^{res}}{\partial x_k}\right)_{T,v,x_{j\neq k}} - \sum\left[y_i\left(\frac{\partial\tilde{a}^{res}}{\partial x_k}\right)_{T,v,x_{i\neq j}}\right] - \ln Z \tag{12}$$

Regular solution models

In recent years, other models have been employed to model solubility in supercritical carbon dioxide, including those related to regular solutions. Unlike equations of state, these models do not require much information about the solvent, but some thermodynamic properties such as the melting point and enthalpy of the APIs are still required. These types of models have been used in many articles[47,70–72]. In the event that supercritical carbon dioxide is regarded as a solvent and the solubility is markedly low, the solubility in $scCO_2$ is derived from the solubility coefficient in the infinitesimal dilute state (γ^{∞}), on the assumption that the fugacity of the API is identical in the two phases of solid and solvent[47,70]:

$$f_{solute}^{S} = f_{solute}^{scCO_2} = f_{solute}^{L} \tag{13}$$

$$y_{solute} = \frac{1}{\gamma^{\infty}}\frac{f_{solute}^{S}}{f_{solute}^{L}} \tag{14}$$

where,

$$\ln\left(\frac{f_{solute}^{S}}{f_{solute}^{L}}\right) = \frac{-\Delta H_m}{R}\left(\frac{1}{T} - \frac{1}{T_m}\right) - \int_{T_m}^{T}\frac{1}{RT^2}\left[\int_{T_m}^{T}\Delta C_p\,dT\right]dT \tag{15}$$

With T_m being melting point and ΔH_m being enthalpy of fusion. If we disregard the discrepancy between the heat capacity ΔH_m of the solute in the solid and supercritical phases (which is nearly constant), then Eq. 15 can be rewritten as follows:[73]:

$$\ln\left(\frac{f_{solute}^{S}}{f_{solute}^{L}}\right) = \frac{-\Delta H_m}{R}\left(\frac{1}{T} - \frac{1}{T_m}\right) + \frac{\Delta C_p}{R}\,ln\left(\frac{T}{T_m}\right) - \frac{\Delta C_p}{RT}\left(\frac{T - T_m}{T}\right) \tag{16}$$

Therefore,

$$y_{solute} = \frac{1}{\gamma^{\infty}}exp\left[\frac{-\Delta H_m}{R}\left(\frac{1}{T} - \frac{1}{T_m}\right) + \frac{\Delta C_p}{R}\,ln\left(\frac{T}{T_m}\right) - \frac{\Delta C_p}{RT}\left(\frac{T - T_m}{T}\right)\right. \tag{17}$$

In this study, the regular solution is employed in conjunction with the Flory-Huggins theory[74] for the purpose of determining γ^{∞}:

$$\ln \gamma^{\infty} = \frac{\nu_{solute}}{RT}\left(\delta_{scCO_2} - \delta_{solute}\right)^2 + 1 - \frac{\nu_{solute}}{\nu_{scCO_2}} + \ln\left(\frac{\nu_{solute}}{\nu_{scCO_2}}\right) \tag{18}$$

In the absence of consideration of the parameter of ΔC_p in Eq. 17, the mole fraction in $scCO_2$ can be determined through the following equation:

$$\ln y_{solute} = \frac{\Delta H_m}{R}\left(\frac{1}{T_m} - \frac{1}{T}\right) - \frac{\nu_{solute}}{RT}\left(\delta_{scCO_2} - \delta_{solute}\right)^2 - 1 + \left(\frac{\nu_{solute}}{\nu_{scCO_2}}\right) - \ln\left(\frac{\nu_{solute}}{\nu_{scCO_2}}\right) \tag{19}$$

Where:

$$\delta_{scCO_2}^2 = \left[\frac{\delta_{dref}}{\left(\frac{\nu_{ref}}{\nu_{scCO_2}}\right)^{-1.25}}\right]^2 + \left[\frac{\delta_{pref}}{\left(\frac{\nu_{ref}}{\nu_{scCO_2}}\right)^{-0.5}}\right]^2 + \left[\frac{\delta_{href}}{\exp\left(-1.32\times10^{-3}\left(T_{ref}-T\right) - \ln\left(\frac{\nu_{ref}}{\nu_{scCO_2}}\right)^{0.5}\right)}\right]^2 \tag{20}$$

$$\delta_{solute} = A + B\rho_{r,\,solvent} \tag{21}$$

$$\delta_{solute} = A + B\rho_{r,\,solvent}^{C} \tag{22}$$

$$\delta_{solute} = A + B\rho_{r,\,solvent} + C\rho_{r,\,solvent}^{2} \tag{23}$$

The A, B, and C were obtained by helping the genetic algorithm. Also, the melting point and enthalpy of fusion were 513.1 K and 29.13 $J.g^{-1}$.

Results and discussions

Table 2 shows the experimental pints for the solubility of sulfasalazine in $scCO_2$ at different pressures (12 to 30 MPa) and temperatures (313 K to 343 K). As previously stated, each data point was replicated three times to ensure the accuracy and precision of the measurements. Additionally, the standard deviation of mole fractions is presented in Table 2. The density of the CO_2 was determined in accordance with the Span-Wagner equation of state. The range of the mole fraction and the solubility of the drug were 2.660×10^{-5} to 1.635×10^{-4} and 0.083 to 1.168 kg/m^3, respectively. The lowest and highest solubilities of sulfasalazine were observed under the highest temperature (343 K) and at the lowest pressure (12 MPa) and the highest pressure (30 MPa), respectively. As illustrated in Fig. 2, the solubility for each of the isotherms was found to increase with rising pressure, and the increase was more pronounced at higher temperatures. This effect is attributed to the increase in spacing of the CO_2 molecules at higher pressures due to the increase in density and performance of carbon dioxide.

Figure 2 illustrates the experimental solubility profile for sulfasalazine at varying temperatures as a function of $ScCO_2$ density and pressure. At a fixed pressure, it becomes evident that two distinct opposing effects of temperature on solubility can be observed: firstly, the CO_2 density, and secondly, the sublimation pressure of the API. The most effective method for elucidating and contrasting these two parameters with regard to solubility is to introduce a parameter designated as the "crossover." This point or range can serve as a valuable reference for comprehending the influence of these two parameters on solubility. A crossover point was identified at 15 MPa, which marked a notable shift in the solubility of the compound under investigation. Moreover, multiple researchers have identified consistent values for the SC-CO_2 crossover region across a range of compounds. These include decitabine ($C_8H_{12}N_4O_4$)[75], aripiprazole ($C_{23}H_{27}Cl_2N_3O_2$)[76], and oxzepam ($C_{23}H_{23}NO_5S$)[77]. Additionally, the same findings were observed for other compounds including hydroxybenzaldehyde ($C_7H_6O_2$)[78], probenecid ($C_{13}H_{19}NO_4S$)[79], gemifloxacin ($C_{18}H_{20}FN_5O_4$)[80] and anthraquinone ($C_{14}H_8O_2$)[81]. At pressures below the crossover point, the value of the solubility exhibited a decline with increasing temperature. Conversely, at pressures above this point, the solubility of the drug demonstrated an increase with rising temperature. A comparable trend was observed for the solubility of other compounds in $ScCO_2$[17,38,59,82,83]. As the temperature increases, the sublimation vapor pressure increases, leading to an increase in solubility. However, it is observed that below the crossover point, as the temperature increases, the density also decreases, resulting in a decrease in solubility. In the other words, at lower pressures, the effect of density becomes more pronounced than that of sublimation pressure, resulting in a decrease in solubility with increasing temperature. At higher pressures (above cross over point), the solubility increases with temperature, indicating that the sublimation pressure effect is the dominant factor. This is to be expected, given that the sublimation pressure increases exponentially with temperature.

Comparison of the correlation results

In this scientific work, an investigation was conducted into a number of different types of models. These models of solubility were created using a variety of approaches, such as, EoS, semi-empirical, and regular solution. As previously stated, each of these models requires a number of input parameters, which were discussed in detail in the preceding sections. In order to facilitate comparison between the models, two criteria were identified and considered: criteria AARD, R_{adj}[8,9].

This work considers a number of density based models, namely Chrastil, Bartle et al., MST, and KJ. Each of the models is underpinned by a comprehensive theoretical framework. The findings from modelling these models are presented in Table 3, and it is evident from this that all of the models demonstrate satisfactory performance. The most precise results were produced by the KJ model with an error rate of 6.12% and a R_{adj} value of 0.994.

Furthermore, ensuring the precise portrayal of data represents a substantial obstacle in the domain of scientific investigation. Nevertheless, it is feasible to determine whether these data align with specific thermodynamic

T (K)[a]	*P* (MPa)	ρ (kg.m^{-3})	y × 10^4	SD (ȳ) × 10^4	S (kg.m^{-3})	Expanded Uncertainty of mole fraction (U×10^5)
313	12	719.2	0.408	0.016	0.266	0.041
	15	781.2	0.44	0.020	0.311	0.042
	18	820.7	0.499	0.021	0.371	0.051
	21	850.4	0.579	0.024	0.446	0.051
	24	873.9	0.712	0.031	0.563	0.074
	27	893.5	0.811	0.036	0.656	0.081
	30	910.3	0.861	0.039	0.710	0.086
318	12	587.2	0.354	0.012	0.188	0.035
	15	701.1	0.464	0.021	0.295	0.046
	18	758.8	0.642	0.029	0.441	0.064
	21	797.4	0.810	0.033	0.585	0.083
	24	826.1	0.974	0.044	0.729	0.097
	27	851.7	1.04	0.047	0.801	0.104
	30	871.5	1.141	0.050	0.900	0.114
328	12	435.3	0.304	0.014	0.120	0.031
	15	606.8	0.499	0.021	0.274	0.050
	18	688.4	0.739	0.031	0.460	0.072
	21	740.3	0.98	0.044	0.657	0.098
	24	777.5	1.181	0.053	0.831	0.119
	27	806.7	1.296	0.054	0.946	0.130
	30	830.5	1.364	0.060	1.025	0.139
338	12	346.1	0.266	0.012	0.083	0.027
	15	507.5	0.499	0.021	0.229	0.050
	18	613.5	0.805	0.033	0.447	0.081
	21	678.9	1.161	0.050	0.714	0.115
	24	724.9	1.319	0.053	0.866	0.134
	27	760.3	1.515	0.064	1.043	0.150
	30	788.9	1.635	0.070	1.168	0.164

Table 2. Solubility values of sulfasalazine.

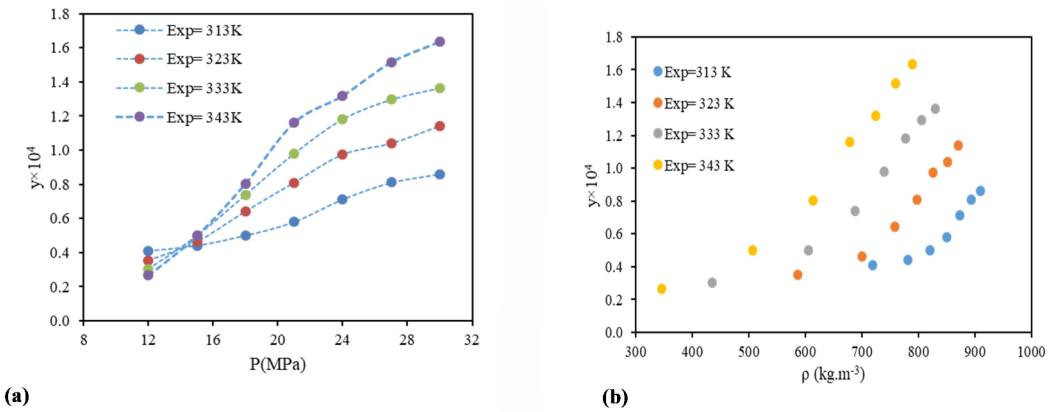

Fig. 2. Solubility data based on pressure (**a**) and density (**b**) at different temperatures.

principles, thereby substantiating their thermodynamic coherence or incoherence. In order to assess the self-consistency of the data, the MST is a frequently employed instrument for the examination of experimental data, with the objective of determining its consistency. In addition to its capacity to correlate data, the ability to extrapolate is a crucial attribute of any model or correlation. Accordingly, the MST (self-consistency test) results were utilized to assess the extrapolation capabilities of the examined models (Fig. 3). As illustrated in Fig. 3, the examined samples exhibited linear trends under all pressures and temperatures, thereby enabling the estimation of data outcomes beyond the present range. Moreover, in accordance with the constants documented in Table 4

Equation	Parameters				Criteria	
	a	b	c	d	AARD (%)	R_{adj}
Chrastil	3.71	-12.92	-4020.3	-	9.22	0.989
Bartle	6497.1	10.55	-6447.3	-	11.92	0.971
KJ	0.445	0.0042	-4203.4	-	6.12	0.994
MST	2.53	13.6	-8464.3	-	7.15	0.991

Table 3. The outcome of the density based models.

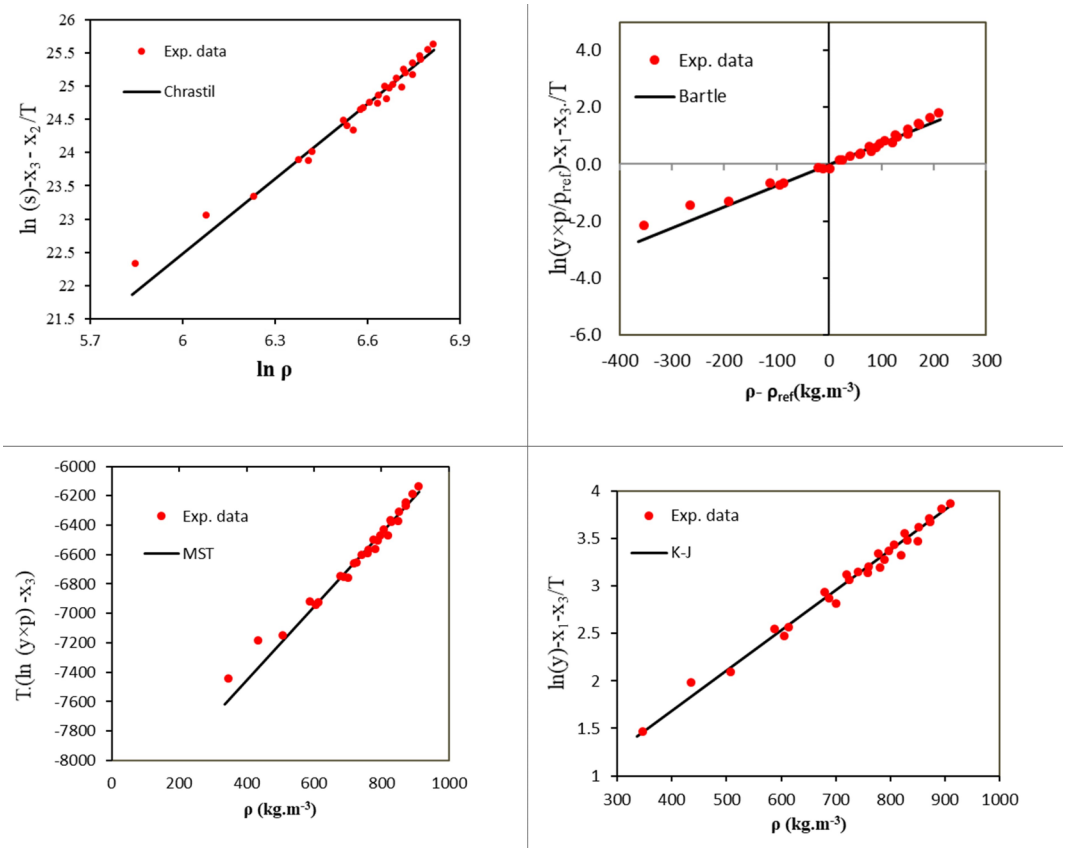

Fig. 3. Consistency solubility data of sulfasalazine.

Compound	ΔH_{total} (kJ mol^{-1}) [a]	$\Delta H_{vap.}$ (kJ mol^{-1})[b]	$\Delta H_{sol.}$ (kJ mol^{-1})[c]
sulfasalazine	33.42	53.60	-20.18

Table 4. The enthalpies for sulfasalazine. [a] Taken from Chrastil model. [b] Taken from Bartle et al., model. [c] The difference between Chrastil and Bartle et al., model.

and the theoretical framework of the models, the enthalpy values of vaporization, solvation, and total were calculated and presented in Table 4.

In this study, Peng Robinson was employed alongside the Van der Waals mixing rule to analyze the data.

In addition, the sublimation vapor pressure associated with each temperature was determined to ensure that accurate comparisons could be made. Prior to using EoS to model solubility, it is of utmost importance to obtain the properties of the solute in question using an appropriate methodology. These properties include, but are not limited to, sublimation pressure, molar volume, critical temperature and pressure, acentric factor, and boiling point. Solubility is subject to several different influences that must be taken into account when modeling solubility. The value of the sublimation pressure depends on the acentric factor, which in turn is significantly influenced by the boiling temperature[84]. Solubility is subject to considerable influence from a number of interdependent factors, the consideration of which is essential when attempting to ascertain the solubility of a given drug. In order to ascertain the critical temperature and pressure, the Marrero-Gani method is employed,

Component	Boiling point (K)	Critical temperature (K)	Critical pressure (MPa)	Acentric factor	Molar volume (cm^3/mol)
Sulfasalazine	844.58[a]	1177.3[a]	1.76[a]	0.495[b]	421.4[c]
P^{sub} (Pa) [d]					
	8.33×10^{-5} (313 K)	3.52×10^{-4} (323 K)	1.36×10^{-3} (333 K)	4.81×10^{-3} (343 K)	

Table 5. Properties of Sulfasalazine. [a] Calculated using Marrero and Gani Method[52]. [b]Ambrose–Walton corresponding states method[85]. [c]Immirzi–Perini method[86]. [d]Grain-Watson method[87].

Model	Parameter	T = 313 K	T = 323 K	T = 333 K	T = 343 K	Overall
PR- vdW2	k_{12}	0.3961	0.3732	0.367	0.3597	
	l_{12}	0.2803	0.2241	0.2003	0.1842	
	$AARD$	5.55	8.50	11.37	11.69	9.27
	R_{adj}	0.9586	0.9402	0.9670	0.9805	0.9615
PC-SAFT	k_{12}	0.095	0.063	0.049	0.025	
	$AARD$	4.55	6.95	7.90	9.84	7.31
	R_{adj}	0.9625	0.9477	0.9761	0.9708	0.9642

Table 6. Correlation results for solubility of sulfasalazine in $ScCO_2$, by PR and PC-SAFT.

which utilises group contributions. Subsequently, the Ambrose-Walton is employed for the calculation of the acentric factor by mentioned information (the critical temperature and pressure obtained). In conclusion, the aforementioned values are employed to ascertain the sublimation pressure via Grain-Watson method at four discrete temperatures (313, 323, 33, and 343 K). The boiling temperatures were determined using the Marrero-Gani while molar volume were calculated using the Immirzi–Perini method, as illustrated in Table 5.

As mentioned above, the Vander Waals mixing rule was used to evaluated the data by PR. The adjustable parameters K_{ij} and L_{ij} as temperature dependent parameters were obtained by AARD. In addition, K_{ij} was considered as a temperature dependent adjustable parameter for PC-SAFT. The intrinsic properties of the API were treated as variables in the PC-SAFT model. The segment diameter (σ), the segment number (m), and the segment energy parameter (ε/k) were estimated to be 4.13, 7.35, and 309 k, respectively, through a process of data fitting. The parameters show an opposite trend to temperature as shown in Table 6. The values of K_{ij} and L_{ij} were presented in Table 6 according to the minimum of AARD. The AARDs were 5.55, 8.50, 11.37 and 11.69 for temperatures of 313, 323, 333, and 343 K, respectively. The ARRD of 4.55, 6.95, 7.90, and 9.84 also reported for PC-SAFT at 313, 323, 333, and 343 K respectively. In addition, R_{adj} for each temperature was 0.9586, 0.9402, 0.9670, and 0.9805 for the PR model and 0.9625, 0.9477, 0.9761, and 0.9708 for the PC-SAFT model. The findings indicated that PC-SAFT and PR were effective in correlating the solubility with a high degree of accuracy, Fig. 4.

The outcomes of the regular solution with three-category solubility parameter calculation are presented in Table 7. The solute solubility parameter (δ_{solute}) is a function of the reduced CO_2 density (ρ_r), which can be expressed using the parameters of A, B, and C. Table 7 shows the values of adjustable parameters for different definitions of δ_{solute} with the statistical parameters of these models. Figure 5 also compares the experimental and the data obtained with these models for different descriptions of δ_{solute}. It is evident that the regular solution, using all given definitions of δ_{solute}, demonstrates an ability to align with the semi-empirical evidence. In consideration of the acquired AARDs, all temperature-independent models exhibit a satisfactory alignment with the data.

Conclusion

The solubility of sulfasalazine (a compound with poor solubility in water) in $scCO_2$ was investigated at seven pressures (12, 15, 18, 21, 24, 27, and 30 MPa) and four temperatures (313, 223, 333, and 343 K). To the best of the authors' knowledge, no previous experimental solubility data exist for this system. In light of the aforementioned considerations, the data presented herein constitute a notable addition to the existing body of literature on the subject. As previously demonstrated, the solubility outcomes exhibited a considerable range, spanning from 0.083 to 1.168 kg/m^3. The minimum and maximum mole fractions were obtained at the highest of the four temperatures utilized in the experiments, namely, 343 K. The maximum measured mole fraction was 2.660×10^{-5} at 12 MPa, and the minimum was 1.635×10^{-4} at 30 MPa. The experimental data were modeled with five density-based models (Chrastil et al., Bartle et al., MST, Kumar-Johnston and, two EoS (PR, and PC-SAFT) and regular solution. The semi-empirical model that yielded the most precise results was that proposed by KJ model, with an absolute relative deviation (AARD) of 6.12% and R_{adj} 0.994. In comparison, the model with the highest AARD (11.92%) was that proposed by Bartle et al. The results are of significant value in the context of an expanding pharmaceutical industry, particularly in light of the ongoing advancement of supercritical technology in this field. It is clear that this and similar research will contribute to the continued growth and development of this field.

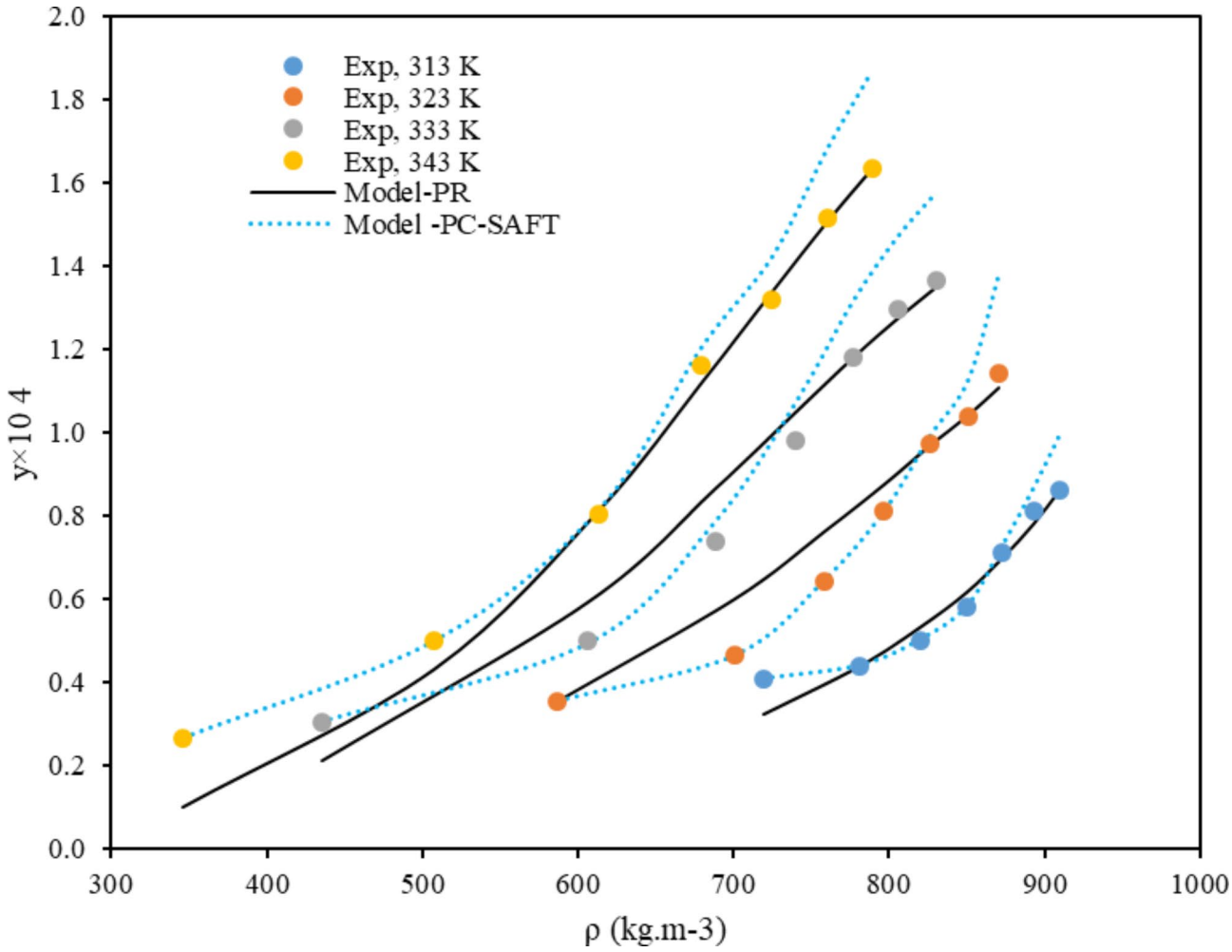

Fig. 4. Modeling by PR and PC-SAFT models.

δ_{solute} based on:	parameters			AARD%	R_{adj}
	A	B	C		
Equation (21)	-8.37	-0.589	-	9.80	0.979
Equation (22)	-6.87	-2.04	0.386	9.32	0.981
Equation (23)	-8.01	-1.044	8.19	9.24	0.982

Table 7. The outcomes of the regular solution method.

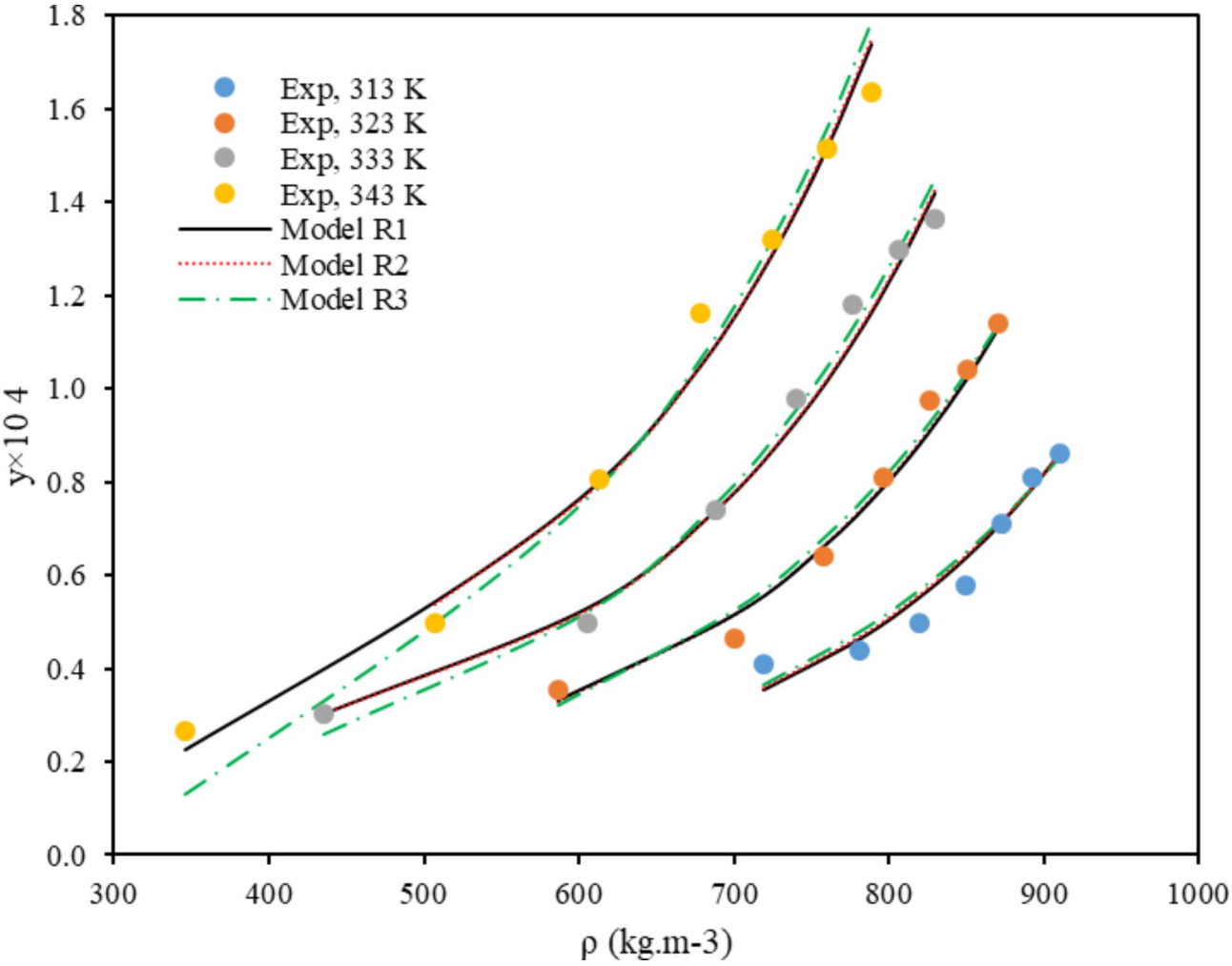

Fig. 5. Modeling by regular solution model.

Data availability

The datasets used and analysed during the current study are available from the corresponding author (Umme Hani) on reasonable request.

Received: 1 September 2024; Accepted: 2 December 2024
Published online: 04 December 2024

References

1. Ol'khovich, M. V., Sharapova, A. V., Blokhina, S. V. & Perlovich, G. L. Sulfasalazine: dissolution and distribution in pharmaceutically relevant mediums. *J. Chem. Eng. Data*. **62**, 123–128 (2017).
2. Shadid, M. et al. Sulfasalazine in ionic liquid form with improved solubility and exposure. *MedChemComm* **6**, 1837–1841 (2015).
3. Esfandiari, N. & Sajadian, S. A. CO2 utilization as Gas Antisolvent for the Pharmaceutical Micro and Nanoparticle production: a review. *Arab. J. Chem.* 104164. (2022).
4. Padrela, L. et al. Supercritical carbon dioxide-based technologies for the production of drug nanoparticles/nanocrystals–a comprehensive review. *Adv. Drug Deliv. Rev.* **131**, 22–78 (2018).
5. Franco P. & De Marco I. Supercritical antisolvent process for pharmaceutical applications: a review. *Processes* **8**, 938 (2020).
6. Gurikov, P. & Smirnova, I. Amorphization of drugs by adsorptive precipitation from supercritical solutions: a review. *J. Supercrit. Fluids*. **132**, 105–125 (2018).
7. Xiang, S. T., Chen, B. Q., Kankala, R. K., Wang, S. B. & Chen, A. Z. Solubility measurement and RESOLV-assisted nanonization of gambogic acid in supercritical carbon dioxide for cancer therapy. *J. Supercrit. Fluids*. **150**, 147–155 (2019).
8. Gahtani, R. M., Talath, S., Hani, U., Rahmathulla, M. & Khalid, A. Pregabalin solubility in supercritical green solvent: a comprehensive experimental and theoretical-intelligent assessment. *J. Mol. Liq.* 125339. (2024).
9. Hani, U. et al. Mathematical optimization and prediction of Febuxostat xanthine oxidase inhibitor solubility through supercritical CO2 system using machine-learning approach. *J. Mol. Liq.* **387**, 122486 (2023).
10. Bartle, K. D., Clifford, A. A., Jafar, S. A. & Shilstone, G. F. Solubilities of solids and liquids of low volatility in supercritical Carbon Dioxide. *J. Phys. Chem. Ref. Data*. **20**, 713–756 (1991).
11. Méndez-Santiago, J. & Teja, A. S. The solubility of solids in supercritical fluids. *Fluid. Phase. Equilibria*. **158**, 501–510 (1999).
12. Mendez-Santiago, J. & Teja, A. S. Solubility of solids in supercritical fluids: consistency of data and a new model for cosolvent systems. *Ind. Eng. Chem. Res.* **39**, 4767–4771 (2000).

13. Chrastil, J. Solubility of solids and liquids in supercritical gases. *J. Phys. Chem.* **86**, 3016–3021 (1982).
14. Kumar, S. K. & Johnston, K. P. Modelling the solubility of solids in supercritical fluids with density as the independent variable. *J. Supercrit. Fluids*. **1**, 15–22 (1988).
15. Garlapati, C. & Madras, G. Solubilities of solids in supercritical fluids using dimensionally consistent modified solvate complex models. *Fluid. Phase. Equilibria*. **283**, 97–101 (2009).
16. Garlapati, C. & Madras, G. New empirical expressions to correlate solubilities of solids in supercritical carbon dioxide. *Thermochim. Acta*. **500**, 123–127 (2010).
17. Alwi, R. S., Garlapati, C. & Tamura, K. Solubility of anthraquinone derivatives in supercritical carbon dioxide: new correlations. *Molecules* **26**, 460 (2021).
18. Del Valle, J. M. & Aguilera, J. M. An improved equation for predicting the solubility of vegetable oils in supercritical carbon dioxide. *Ind. Eng. Chem. Res.* **27**, 1551–1553 (1988).
19. Sung, H. D. & Shim, J. J. Solubility of C. I. disperse Red 60 and C. I. disperse Blue 60 in supercritical Carbon Dioxide. *J. Chem. Eng. Data*. **44**, 985–989 (1999).
20. Adachi, Y. & Lu, B. C. Y. Supercritical fluid extraction with carbon dioxide and ethylene. *Fluid. Phase. Equilibria*. **14**, 147–156 (1983).
21. Bian, X. Q., Zhang, Q., Du, Z. M., Chen, J. & Jaubert, J. N. A five-parameter empirical model for correlating the solubility of solid compounds in supercritical carbon dioxide. *Fluid. Phase. Equilibria*. **411**, 74–80 (2016).
22. Bian, X., Du, Z. & Tang, Y. An improved density-based model for the solubility of some compounds in supercritical carbon dioxide. *Thermochim. Acta*. **519**, 16–21 (2011).
23. Sparks, D. L., Hernandez, R. & Estévez, L. A. Evaluation of density-based models for the solubility of solids in supercritical carbon dioxide and formulation of a new model. *Chem. Eng. Sci.* **63**, 4292–4301 (2008).
24. Si-Moussa, C., Belghait, A., Khaouane, L., Hanini, S. & Halilali, A. Novel density-based model for the correlation of solid drugs solubility in supercritical carbon dioxide. *C. R. Chim.* (2016).
25. Belghait, A., Si-Moussa, C., Laidi, M. & Hanini, S. Semi-empirical correlation of solid solute solubility in supercritical carbon dioxide: comparative study and proposition of a novel density-based model. *C. R. Chim.* **21**, 494–513 (2018).
26. Amooey, A. A. A simple correlation to predict drug solubility in supercritical carbon dioxide. *Fluid. Phase. Equilibria*. **375**, 332–339 (2014).
27. Haghbakhsh, R., Hayer, H., Saidi, M., Keshtkari, S. & Esmaeilzadeh, F. Density estimation of pure carbon dioxide at supercritical region and estimation solubility of solid compounds in supercritical carbon dioxide: correlation approach based on sensitivity analysis. *Fluid. Phase. Equilibria*. **342**, 31–41 (2013).
28. Mitra, S. & Wilson, N. K. An empirical method to predict solubility in supercritical fluids. *J. Chromatogr. Sci.* **29**, 305–309 (1991).
29. Reddy, T. A. & Garlapati, C. Dimensionless empirical model to correlate pharmaceutical compound solubility in supercritical carbon dioxide. *Chem. Eng. Technol.* **42**, 2621–2630 (2019).
30. Tippana Ashok, R. S., Reddy, C. & Garlapati A new empirical model to correlate solubility of pharmaceutical compounds in supercritical carbon dioxide. *J. Appl. Sci. Eng. Methodologies*. **4**, 575–590 (2018).
31. Gordillo, M., Blanco, M., Molero, A. & De La Ossa, E. M. Solubility of the antibiotic penicillin G in supercritical carbon dioxide. *J. Supercrit. Fluids*. **15**, 183–190 (1999).
32. Sodeifian, G., Sajadian, S. A., Razmimanesh, F. & Hazaveie, S. M. Solubility of Ketoconazole (antifungal drug) in SC-CO2 for binary and ternary systems: measurements and empirical correlations. *Sci. Rep.* **11**, 1–13 (2021).
33. Sodeifian, G., Razmimanesh, F. & Sajadian, S. A. Solubility measurement of a chemotherapeutic agent (Imatinib mesylate) in supercritical carbon dioxide: Assessment of new empirical model. *J. Supercrit. Fluids*. **146**, 89–99 (2019).
34. Sodeifian, G., Nateghi, H. & Razmimanesh, F. Measurement and modeling of dapagliflozin propanediol monohydrate (an anti-diabetes medicine) solubility in supercritical CO2: evaluation of new model. *J. CO2 Utilization*. **80**, 102687 (2024).
35. Pishnamazi, M. et al. Using static method to measure tolmetin solubility at different pressures and temperatures in supercritical carbon dioxide. *Sci. Rep.* **10**, 1–7 (2020).
36. Pishnamazi, M. et al. Measuring solubility of a chemotherapy-anti cancer drug (busulfan) in supercritical carbon dioxide. *J. Mol. Liq.* **317**, 113954 (2020).
37. Zabihi, S. et al. Thermodynamic study on solubility of brain tumor drug in supercritical solvent: Temozolomide case study. *J. Mol. Liq.* **321**, 114926 (2021).
38. Pishnamazi, M. et al. Chloroquine (antimalaria medication with anti SARS-CoV activity) solubility in supercritical carbon dioxide. *J. Mol. Liq.* **322**, 114539 (2021).
39. Bartle, K., Clifford, A., Jafar, S. & Shilstone, G. Solubilities of solids and liquids of low volatility in supercritical carbon dioxide. *J. Phys. Chem. Ref. Data*. **20**, 713–756 (1991).
40. Ardestani, N. S., Sajadian, S. A., Esfandiari, N., Rojas, A. & Garlapati, C. Experimental and modeling of solubility of sitagliptin phosphate, in supercritical carbon dioxide: proposing a new association model. *Sci. Rep.* **13**, 17506 (2023).
41. Sajadian, S. A., Ardestani, N. S., Esfandiari, N., Askarizadeh, M. & Jouyban, A. Solubility of favipiravir (as an anti-COVID-19) in supercritical carbon dioxide: an experimental analysis and thermodynamic modeling. *J. Supercrit. Fluids* 105539. (2022).
42. Esfandiari, N. & Sajadian, S. A. Experimental and modeling investigation of Glibenclamide Solubility in Supercritical Carbon dioxide. *Fluid. Phase. Equilibria* 113408. (2022).
43. Sajadian, S. A., Ardestani, N. S. & Jouyban, A. Solubility of montelukast (as a potential treatment of COVID-19) in supercritical carbon dioxide: experimental data and modelling. *J. Mol. Liq.* **349**, 118219 (2022).
44. Anitha, N. & Chandrasekhar, G. A simple model to correlate solubility of thermolabile solids in supercritical fluids, in: AIP Conference Proceedings, AIP Publishing, (2022).
45. Yan, J. et al. Comparison of Four Density-Based Semi-Empirical Models for the Solubility of Azo Disperse Dyes in Supercritical Carbon Dioxide, Processes. 10 1960. (2022).
46. Nguyen, H. C. et al. Computational prediction of drug solubility in supercritical carbon dioxide: thermodynamic and artificial intelligence modeling. *J. Mol. Liq.* **354**, 118888 (2022).
47. Abourehab, M. A. S. et al. Laboratory determination and thermodynamic analysis of Alendronate Solubility in Supercritical Carbon Dioxide. *J. Mol. Liq.* 120242. (2022).
48. Razmimanesh, F., Sodeifian, G. & Sajadian, S. A. An investigation into Sunitinib malate nanoparticle production by US-RESOLV method: Effect of type of polymer on dissolution rate and particle size distribution. *J. Supercrit. Fluids*. **170**, 105163 (2021).
49. Sodeifian, G., Sajadian, S. A. & Derakhsheshpour, R. Experimental measurement and thermodynamic modeling of Lansoprazole solubility in supercritical carbon dioxide: application of SAFT-VR EoS. *Fluid. Phase. Equilibria*. **507**, 112422 (2020).
50. Sodeifian, G., Saadati Ardestani, N., Sajadian, S. A., Golmohammadi, M. R. & Fazlali, A. Prediction of solubility of Sodium Valproate in Supercritical Carbon Dioxide: experimental study and thermodynamic modeling. *J. Chem. Eng. Data*. **65**, 1747–1760 (2020).
51. Joback, K. G., Reid, R. C. & ESTIMATION OF PURE-COMPONENT PROPERTIES FROM GROUP-CONTRIBUTIONS. *Chem. Eng. Commun.* **57** 233–243. (1987).
52. Marrero, J. & Gani, R. Group-contribution based estimation of pure component properties. *Fluid. Phase. Equilibria*. **183**, 183–208 (2001).
53. Lee, B. I. & Kesler, M. G. A generalized thermodynamic correlation based on three-parameter corresponding states. *AIChE J.* **21**, 510–527 (1975).

54. Fedors, R. F. A method for estimating both the solubility parameters and molar volumes of liquids. *Polym. Eng. Sci.* **14**, 147–154 (1974).
55. Stein, S. E. & Brown, R. L. Estimation of normal boiling points from group contributions. *J. Chem. Inform. Comput. Sci.* **34**, 581–587 (1994).
56. Sodeifian, G., Drakhsheshpoor, R. & Sajadian, S. A. Experimental study and thermodynamic modeling of Esomeprazole (proton-pump inhibitor drug for stomach acid reduction) solubility in supercritical carbon dioxide. *J. Supercrit. Fluids* 104606. (2019).
57. Sodeifian, G., Razmimanesh, F., Sajadian, S. A., Soltani, H. & Panah Solubility measurement of an antihistamine drug (loratadine) in supercritical carbon dioxide: Assessment of qCPA and PCP-SAFT equations of state. *Fluid. Phase. Equilibria*. **472**, 147–159 (2018).
58. Sodeifian, G., Razmimanesh, F. & Sajadian, S. A. Prediction of solubility of sunitinib malate (an anti-cancer drug) in supercritical carbon dioxide (SC–CO2): experimental correlations and thermodynamic modeling. *J. Mol. Liq.* 111740. (2019).
59. Morales-Díaz, C., Cabrera, A. L., Juan, C. & Mejía, A. Modelling of solubility of vitamin K3 derivatives in supercritical carbon dioxide using cubic and SAFT equations of state. *J. Supercrit. Fluids*. **167**, 105040 (2021).
60. Sodeifian, G., Razmimanesh, F., Sajadian, S. A. & Panah, H. S. Solubility measurement of an antihistamine drug (loratadine) in supercritical carbon dioxide: Assessment of qCPA and PCP-SAFT equations of state. *Fluid. Phase. Equilibria*. **472**, 147–159 (2018).
61. Hosseini Anvari, M. & Pazuki, G. A study on the predictive capability of the SAFT-VR equation of state for solubility of solids in supercritical CO2. *J. Supercrit. Fluids*. **90**, 73–83 (2014).
62. Abdallah, A. E., Si-Moussa, C., Hanini, S. & Laidi, M. Application of PC-SAFT and cubic equations of state for the correlation of solubility of some pharmaceutical and statin drugs in SC-CO2. *Chem. Ind. Chem. Eng. Q.* **19**, 449–460 (2013).
63. McCabe, C. & Galindo, A. SAFT associating fluids and fluid mixtures. *Appl. Thermodyn. Fluids* 215–279. (2010).
64. Gross, J. & Sadowski, G. Perturbed-chain SAFT: an equation of state based on a perturbation theory for chain molecules. *Ind. Eng. Chem. Res.* **40**, 1244–1260 (2001).
65. McCabe, C., Galindo, A., García-Lisbona, M. N. & Jackson, G. Examining the adsorption (vapor – liquid equilibria) of short-chain hydrocarbons in low-density polyethylene with the SAFT-VR approach. *Ind. Eng. Chem. Res.* **40**, 3835–3842 (2001).
66. McCabe, C. & Jackson, G. SAFT-VR modelling of the phase equilibrium of long-chain n-alkanes. *Phys. Chem. Chem. Phys.* **1**, 2057–2064 (1999).
67. Smith, J. M. Introduction to chemical engineering thermodynamics. in, *ACS Publications*, (1950).
68. Ali Sajadian, S., Amani, M., Saadati Ardestani, N. & Shirazian, S. Experimental analysis and thermodynamic modelling of Lenalidomide Solubility in Supercritical Carbon Dioxide. *Arab. J. Chem.* 103821. (2022).
69. Gross, J. & Sadowski, G. Application of perturbation theory to a hard-chain reference fluid: an equation of state for square-well chains. *Fluid. Phase. Equilibria*. **168**, 183–199 (2000).
70. Esfandiari, N. et al. Solubility measurement of verapamil for the preparation of developed nanomedicines using supercritical fluid. *Sci. Rep.* **13**, 17089 (2023).
71. Sodeifian, G., Alwi, R. S., Razmimanesh, F. & Abadian, M. Solubility of Dasatinib monohydrate (anticancer drug) in supercritical CO2: experimental and thermodynamic modeling. *J. Mol. Liq.* **346**, 117899 (2022).
72. Sodeifian, G., Alwi, R. S., Razmimanesh, F. & Roshanghias, A. Solubility of pazopanib hydrochloride (PZH, anticancer drug) in supercritical CO2: experimental and thermodynamic modeling. *J. Supercrit. Fluids*. **190**, 105759 (2022).
73. Nasri, L. Modified Wilson's model for correlating solubilities in supercritical fluids of some polycyclic aromatic solutes. *Polycycl. Aromat. Compd.* **38**, 244–256 (2018).
74. Cheng, J. S., Tang, M. & Chen, Y. P. Correlation of solid solubility for biological compounds in supercritical carbon dioxide: comparative study using solution model and other approaches. *Fluid. Phase. Equilibria*. **194**, 483–491 (2002).
75. Pishnamazi, M. et al. Experimental and thermodynamic modeling decitabine anti cancer drug solubility in supercritical carbon dioxide. *Sci. Rep.* **11**, 1075 (2021).
76. Ansari, E., Honarvar, B., Sajadian, S. A., Aboosadi, Z. A. & Azizi, M. *Solubility of Aripiprazole in Supercritical Carbon Dioxide* (Experimental and modeling evaluations, 2023).
77. Rojas, A. et al. Solubility of oxazepam in supercritical carbon dioxide: experimental and modeling. *Fluid. Phase. Equilibria* 114165. (2024).
78. Jin, J., Wang, Y., Zhang, H., Fan, X. & Wu, H. Solubility of 4-hydroxybenzaldehyde in supercritical carbon dioxide with and without cosolvents. *J. Chem. Eng. Data*. **59**, 1521–1527 (2014).
79. Khudaida, S. H. et al. Solubility of probenecid in supercritical carbon dioxide and composite particles prepared using supercritical antisolvent process. *J. Supercrit. Fluids*. **194**, 105851 (2023).
80. Arabgol, F., Amani, M., Ardestani, N. S. & Sajadian, S. A. Experimental and thermodynamic investigation of gemifloxacin solubility in supercritical CO2 for the production of nanoparticles. *J. Supercrit. Fluids*. **206**, 106165 (2024).
81. Alwi, R. S. & Tamura, K. Measurement and correlation of derivatized anthraquinone solubility in supercritical carbon dioxide. *J. Chem. Eng. Data*. **60**, 3046–3052 (2015).
82. Sodeifian, G., Garlapati, C., Razmimanesh, F. & Sodeifian, F. Solubility of amlodipine besylate (calcium channel blocker drug) in supercritical carbon dioxide: measurement and correlations. *J. Chem. Eng. Data*. **66**, 1119–1131 (2021).
83. Sodeifian, G., Garlapati, C., Razmimanesh, F. & Sodeifian, F. The solubility of Sulfabenzamide (an antibacterial drug) in supercritical carbon dioxide: evaluation of a new thermodynamic model. *J. Mol. Liq.* **335**, 116446 (2021).
84. Poling, B. E. & Prausnitz, J. M. J.P. O'connell, The properties of gases and liquids, Mcgraw-hill New York, (2001).
85. Poling, B. E., Prausnitz, J. M., Paul, J. & Reid, O. C. *R.C., the Properties of Gases and Liquids* (McGraw-Hill New York, 2001).
86. Immirzi, A. & Perini, B. Prediction of density in organic crystals. *Acta Crystallogr. Sect. A*. **33**, 216–218 (1977).
87. Morales-Díaz, C., Cabrera, A. L., de la Fuente, J. C. & Mejía, A. Modelling of solubility of vitamin K3 derivatives in supercritical carbon dioxide using cubic and SAFT equations of state. *J. Supercrit. Fluids*. **167**, 105040 (2021).

Acknowledgements

The authors extend their sincere appreciation to the Deanship of Scientific Research at King Khalid University for funding this work through Large Research Group. Under the grant number RGP2/150/45.

Author contributions

Y.A. : Writing, drafting. editing, formal analysis, validation, conceptualization, supervisionM.G.: Writing, drafting. editing, modeling, resourcesS.T.: Writing, drafting. editing, investigation, analysisA.W.: Writing, drafting. editing, resources, analysis, modelingS.B.S.: Writing, drafting. editing, investigation, formal analysisF.F.: Writing, drafting. editing, resources, analysis, modelingU.H.: Writing, supervision, editing, validation, analysis, modeling.

Declarations

Competing interests
The authors declare no competing interests.

Additional information
Correspondence and requests for materials should be addressed to U.H.

Reprints and permissions information is available at www.nature.com/reprints.

Publisher's note Springer Nature remains neutral with regard to jurisdictional claims in published maps and institutional affiliations.